Published in final edited form as:
Acta Neuropathol. 2009 September ; 118(3): 415–428. doi:10.1007/s00401-009-0546-8.

Wolfram syndrome: a clinicopathologic correlation

Justin B. Hilson,
Department of Pathology, Beth Israel Deaconess Medical, Center, Harvard Medical School, 330 Brookline Ave, Boston, MA 02215, USA, jhilson@bidmc.harvard.edu

Saumil N. Merchant,
Department of Otology and Laryngology, Massachusetts Eye, and Ear Infirmary, Harvard Medical School, Boston, MA, USA

Joe C. Adams, and
Department of Otology and Laryngology, Massachusetts Eye, and Ear Infirmary, Harvard Medical School, Boston, MA, USA

Jeffrey T. Joseph
Department of Pathology, University of Calgary, Calgary, AB, Canada

Abstract

Wolfram syndrome or DIDMOAD (diabetes insipidus, diabetes mellitus, optic atrophy and deafness) is a neurodegenerative disorder characterized by diabetes mellitus and optic atrophy as well as diabetes insipidus and deafness in many cases. We report the post-mortem neuropathologic findings of a patient with Wolfram syndrome and correlate them with his clinical presentation. In the hypothalamus, neurons in the paraventricular and supraoptic nuclei were markedly decreased and minimal neurohypophyseal tissue remained in the pituitary. The pontine base and inferior olivary nucleus showed gross shrinkage and neuron loss, while the cerebellum was relatively unaffected. The visual system had moderate to marked loss of retinal ganglion neurons, commensurate loss of myelinated axons in the optic nerve, chiasm and tract, and neuron loss in the lateral geniculate nucleus but preservation of the primary visual cortex. The patient's inner ear showed loss of the organ of Corti in the basal turn of the cochleae and mild focal atrophy of the stria vascularis. These findings correlated well with the patient's high-frequency hearing loss. The pathologic findings correlated closely with the patient's clinical symptoms and further support the concept of Wolfram syndrome as a neurodegenerative disorder. Our findings extend prior neuropathologic reports of Wolfram syndrome by providing contributions to our understanding of eye, inner ear and olivopontine pathology in this disease.

Keywords

Wolfram syndrome; DIDMOAD; Neuropathology; Otopathology

Introduction

Wolfram syndrome was first described in 1938 by Wolfram and Wagener [31] as a hereditary syndrome characterized by diabetes mellitus and optic atrophy acquired early in life. Subsequent reports added diabetes insipidus and deafness to the syndrome, which develop in approximately 73 and 62% of sufferers, respectively [1,26]. These features have led to the

Correspondence to: Justin B. Hilson.

alternative acronym, DIDMOAD (diabetes insipidus, diabetes mellitus, optic atrophy and deafness), to describe the disease and approximately 50% suffer from the full phenotype. Additional studies have expanded the list of possible symptoms to include a wide variety of neurological manifestations, including psychiatric illness [22]. Affected individuals have a median age at death of 30, usually from central respiratory failure [6].

Genetic studies have shown that the mutations of the WFS1 gene on chromosome 4 are responsible for the symptoms of Wolfram syndrome in the majority of cases (90%) [9,20,25]. This gene putatively encodes an endoplasmic reticulum membrane protein (wolframin) found in neurons and pancreatic β-cells as well as other tissues including the heart, placenta, inner ear, lung and liver. The function of wolframin is unknown; however, deficiencies in the protein are believed to increase stress within the endoplasmic reticulum, impair the cell cycle and affect calcium homeostasis [26,32].

Brain imaging of patients with Wolfram syndrome has demonstrated atrophy of the optic tracts, hypothalamus and posterior pituitary in all patients. Cerebellum, cerebral cortex and upper brainstem atrophy is variable [7,26]. These findings all suggest a central multisystem neurodegenerative process rather than a congenital disease.

The few neuropathological studies of Wolfram syndrome patients report atrophy of the optic nerves, tract and chiasm, and the lateral geniculate nucleus [2,7,23]. Loss of fibers in the cochlear nerve and loss of neurons in the paraventricular and supraoptic nuclei of the hypothalamus are consistent findings [6,22,23]. Numerous other reported lesions include gliosis and atrophy of the olfactory bulbs, cerebellum, dorsomedial and anterior thalamic nuclei, neuronal loss from the substantia nigra and a case of corpus callosum agenesis [23]. Taken together, these findings further support a diffuse neurodegenerative process, having a remarkable diversity in presentation. In this study, we report the neuropathologic findings in a patient with Wolfram syndrome, which provides unique descriptions of ear, pituitary and retina pathology as well as provides additional evidence to support a neurodegenerative process.

Case report

The patient was a 24-year-old man who first experienced symptoms at an age of 6 years, when he developed color blindness. Three years later he started to complain of progressive vision loss. That same year he also presented with diabetes insipidus. By age 12, he had developed diabetes mellitus requiring life-long insulin therapy. His thyroid was removed at age 11 due to a diagnosis of Hashimoto's thyroiditis. He also suffered from clinical depression and occasional bouts of suicidal ideation. In the years immediately preceding his death, his visual acuity had deteriorated to the point where he was completely blind to all but bright light. Fundoscopy showed very pale optic discs. He had prominent gaze-evoked nystagmus bilaterally and his pursuit and vestibular–ocular reflex cancellation were mildly impaired. The patient suffered from hearing loss (unknown year of onset); an audiogram at age 12 showed high-tone sensorineural hearing loss (SNHL) (see Fig. 7a, b). Hearing aids were fitted at age 16, but were minimally helpful and ultimately discontinued. Speech discrimination was essentially normal. His language was normal, but he had a slurred dysarthria. He had no history of otorrhea or ear infections and otoscopic examinations of both ears were normal. Neurological exam revealed normal finger–nose coordination and rapid alternating movements. His one-foot stance was impaired, as was his tandem gait forward and backward. An MRI scan found mild cerebral and cerebellar atrophy, inappropriate for the patient's age, but without focal intrinsic abnormalities in the brain. Imaging also showed mild atrophic changes in the pons and probable mild atrophy of the optic nerves. He had been educated at a school for the blind and at the time of his death he was living in an assisted living facility and employed at a local

grocery store. In the year before his death, he developed methicillin-resistant *Staphylococcus aureus* and *Pseudomonas* pneumonia and seizures following an overdose of insulin. Subsequently, he had repeated episodes of pneumonia that were, in part, due to aspiration. He also had episodes of unresponsiveness, possibly from central hypoventilation. In the weeks immediately prior to his death, he was hospitalized for an aspiration pneumonia that was cultured positive for methicillin resistant *S. aureus*. His condition required mechanical ventilation after which his pulmonary condition deteriorated until he succumbed to complications of adult respiratory distress syndrome.

Methods

Permission for autopsy and use of tissues for research was obtained from the patient's parents. We obtained the brain, spinal cord and posterior aspects of his eyes for examination. Brain tissue for microscopic examination was fixed in formalin, paraffin embedded, sectioned and stained with either hematoxylin and eosin (H&E) or hematoxylin and eosin/Luxol-fast blue (LFB) for light microscopy. On selected sections, immunohistochemical staining for adrenocorticotropic hormone (Dako 02A3, 1:24), growth hormone (Dako, 1:25), follicle-stimulating hormone (Dako, 1:100), luteinizing hormone (Dako C93, 1:50), thyroid-stimulating hormone (Dako 42, 1:200), prolactin (Dako, 1:800), glial fibrillary acidic protein (GFAP, Dako, 1:4000), neurofilament protein (NF, Biogenex, 1:4,000), calretinin (Invitrogen, 1:100), and NeuN (Chemicon, 1:40) was performed. Bielschowsky staining was also performed on selected sections.

Both temporal bones, including the inner ears, were removed at 15 h postmortem and processed in celloidin for light microscopy [24]. All serial sections through both cochleae were used to quantitatively assess for loss of neurosensory elements including outer hair cells, inner hair cells, stria vascularis and cochlear neuronal cells, using the method described by Schuknecht [24].

Sections of the patient's retina had become detached during the autopsy and so could not be mapped precisely to a control retina. To facilitate comparison with a control retina, the width of the rod cell layers were equalized in Fig. 4a, b.

In order to obtain maximum resolution and contrast in microscopic images, several images in the figures (Fig. 5b, c, Fig. 6b) were prepared by photographing over-lapping micrographs at higher magnification and then merging them into a single larger image using the Photo-merge function in Adobe Photoshop. Adobe Photoshop was also used to map the areas of greatest injury in pons (Fig. 8e). These areas had a distinct color profile that allowed them to be selected using the "Color Range" option in the Selection menu. The regions identified were then compared to the routine light microscopy to confirm the mapping.

Results

Pancreas

On H&E stains, the pancreas had a normal acinar architecture, but lacked islets (Fig. 1a). This was confirmed by the nearly complete absence of synaptophysin staining (Fig. 1b), indicating a total or near total loss of insulin-producing islets cells.

Gross brain findings

The brain weighed 1,100 g before fixation. Externally, the entire brainstem was small, especially in comparison with its relatively normal cranial nerves (Fig. 2a). The optic nerve (II, Fig. 2a) was gray rather than white and shrunken to the size of the oculomotor nerve (III, Fig. 2a). The olfactory tracts and bulbs were normal in size (not shown). The pontine base was

approximately two-thirds of normal (black arrowheads, Fig. 2a, b), while the pontine tegmentum was relatively spared (Fig. 2b). The medulla had only minimal olivary surface bulges (white arrows, Fig. 2a) and was reduced in width (Fig. 2c). In addition, the medullary reticular formation (RF, Fig. 2c) was small. Brainstem cranial nerves were normal. Dissection of the cerebrum was essentially normal, except that the lateral geniculate nucleus was pale (Fig. 2e) rather than its normal orange-brown color (Fig. 2d). The remaining cerebral cortex, basal ganglia and thalamus were not atrophic or discolored and the ventricular system was not dilated (Fig. 2f). Within the primary visual cortex, the line of Gennari was distinct (data not shown). The volume of the middle cerebellar peduncle was diminished (see Fig. 2a), while the cerebellar folia and dentate nucleus showed no significant atrophy or discoloration (Fig. 2g).

Hypothalamic–pituitary axis

Correlating with the patient's diabetes insipidus, the hypothalamus showed significant neuron loss and gliosis in the paraventricular and supraoptic nucleus (Fig. 3a, b1, b2). The remainder of the hypothalamus, including the mammillary bodies, fornix, subfornical organ and dorsolateral hypothalamus, was histologically normal.

Sectioning through multiple levels of the entire pituitary gland failed to reveal significant neurohypophyseal tissue (Fig. 3c). Only a thin rim of neuroglial tissue remained on the posterior pituitary, as identified on GFAP immunostains (Fig. 3d). Most of the adenohypophysis was structurally normal; a small focus lacked a normal nested architecture but showed several cell types (Fig. 4c, e). Immunohistochemical staining for adrenocorticotrophic hormone (ACTH), growth hormone (GH), follicle-stimulating hormone (FSH), luteinizing hormone (LH), thyroid-stimulating hormone (TSH) and prolactin stained individual cells in both the structurally intact and amorphous areas (data not shown).

Visual system

The patient's visual system was severely affected. The optic nerves and tracts were shrunken and gray (see above). The lateral geniculate nucleus was also small, yellow-gray, and had lost its normal striped pattern (Fig. 2d, e).

The posterior retina demonstrated a moderate to marked loss of the retinal ganglion neurons and slight vacuolization of the retinal ganglion cell layer (compare Fig. 4a, b). Unlike the outer nuclear layer, which was relatively preserved, the inner nuclear layer was thin. Both the internal and external plexiform layers were also significantly reduced in width. Calretinin immunostains showed occasional cells at the outer edge of the ganglion cell layer (arrowhead, Fig. 4c) and sporadic positive cells in the inner zone of the inner plexiform layer (arrows, Fig. 4c). Based on their location and staining, these likely represent amacrine AII cells [4, 30] although we cannot entirely exclude that they are displaced ganglion cells. A few retinal ganglion neurons showed light calretinin staining (data not shown). Neu-N immunostains (Fig. 4d) revealed a few more neurons in the ganglion cell layer than H&E; many of these were flattened or shrunkened. The few remaining ganglion neurons on routine stains were not enlarged, although ganglion swelling could not be excluded, given the small sample that remained.

Retinal projections had undergone corresponding axonal degeneration and showed a moderate to marked loss of myelinated axons with secondary gliosis in the optic nerve (Fig. 4e), chiasm and tract (see Fig. 3a). Calretinin immunoperoxidase lightly stained the sparse axons within the optic nerve (Fig. 4f); these stains did not demonstrate large axonal spheroids. The axon loss in the optic tract was variable, with near complete loss centrally and with relative preservation at the periphery (OT in Fig. 3a).

Much of the normal architecture of the lateral geniculate nucleus (LGN, Fig. 5a) had been effaced by the loss of the retinal projections, its marked neuronal loss and the consequent axonal degeneration in the optic radiation. In coronal sections at the level of the posterior commissure, the LGN lies just medial to the attachment point of the choroid plexus ("ap" in Fig. 5a) and is surrounded on all sides by myelinated axons, including on its border with the brain exterior (see myelin boundary, mb, of control in inset of Fig. 5a). These two landmarks were used to confirm the location of the denuded LGN. Detailed microscopy of this region demonstrated a residual myelin boundary ("mb", Fig. 5b) and few remaining LGN magnocellular neurons immediately superior to this structure ("MCN", Fig. 5c). The origin of the optic radiation immediately superior to the LGN was devoid of a meaningful number of myelinated axons ("or" and open arrowhead, Fig. 5b).

The primary visual cortex had a distinct macroscopic stria of Gennari (data not shown). This was confirmed by microscopy, which showed a well-myelinated line of Gennari along the entire section of area 17 (Fig. 6a). This myelinated line is the most pronounced example of the outer band of Baillarger common to most types of neocortex. In area 17, this band lies in layer IV-B (see Fig. 6b), which receives its major inputs from other areas of cortex but not from the LGN [15]. Its thinly myelinated fibers likely represent intrinsic cortical axonal connections. The LGN projects mainly to layer IV-C, which typically has sparse myelin staining as in this patient (Fig. 6b) [15,16]. In the occipital lobe, the effect of the marked loss of neurons in the LGN is reflected in the pallor and gliosis in the optic radiation ("or", Fig. 6a). No swollen neurons, axonal spheroids or myelin ovoids were identified on myelin (Fig. 6c) or axon silver (Fig. 6d) stains. Within the limitations of autopsy material and this analysis, the patient's primary visual cortex was structurally normal.

Auditory system

Both cochleae were fully developed and showed the typical basal, middle and apical turns (Fig. 7c). There was complete atrophy of the organ of Corti in the lower basal turn (0–14 mm on the right and 0–13 mm on the left) where inner hair cells, outer hair cells and supporting cells were missing (Fig. 7d). Beyond this region, there was a fairly abrupt transition to a healthy-appearing organ of Corti with the presence of pillar cells, supporting cells and inner hair cells. Outer hair cells were partially missing in the next few millimeters (14–18 mm on the right and 13–18 mm on the left), beyond which the organ of Corti was completely intact on both sides (Fig. 7e). The tonotopic distribution of loss of hair cells corresponded well with the high-frequency hearing loss observed on audiometric testing (Fig. 7a, b). The stria vascularis was generally intact in both ears except for small areas of focal atrophy in the apical turn (Fig. 7a, b). Overall, cochlear neurons were intact except in the proximal basal turn where some of the cell bodies had degenerated (Fig. 7d). The cochlear nerve and the vestibular sense organs were intact. Numerous osteoclasts had accumulated along the anterior and lateral wall of the bony eustachian tube. They were present at the junction of the submucosa and bone, and appeared to be actively resorbing the underlying bone. The dorsal and ventral cochlear nuclei and primary auditory cortex (Heschl's gyrus) were essentially normal.

Olivopontocerebellar system

On gross examination, the medulla and pons were shrunken (see above), while the cerebellum was largely unaffected. The small size of these structures was due in part to degeneration of extant neurons, as evidenced by the presence of gliotic gray matter neuropil devoid of neurons. Regions showing gliosis and neuron loss included the medial vestibular nucleus (not further discussed), medullary reticular formation, inferior olivary nucleus (ION) and the pontine base. Comparison of approximately the same level of the medulla (Fig. 8a) and pons (Fig. 8d), of the patient and a control confirms the gross findings: the ION and medullary reticular formation

("RF") are smaller in the medulla (Fig. 8a) and the base, but not the tegmentum, which was smaller in the pons (Fig. 8d).

Neurons were moderately decreased in the ION (Fig. 8b). While many neurons remain, they are more spread out than in controls. In cross-sections taken at approximately the same level of the medulla, the ION had only about one-third of the neurons as the control (321 compared to 887). Although some remaining neurons were clustered, the neuron loss was diffuse and not patchy. The remaining neurons immunoreacted with calretinin antibodies (data not shown). While a few swollen axons in the hilum of the ION were highlighted with APP stains (Fig. 8c), these were rare; most did not stain. The ION projects into the cerebellum through the medial aspect of the inferior cerebellar peduncle (ICP); this region showed only mild myelin pallor compared to the remainder of the ICP (data not shown), indicating that the remaining neurons likely maintained their connections with cerebellar Purkinje neurons. Increased gliosis and decreased myelinated axons affected the dorsal and lateral reticular nuclei and the intermediate reticular zone; the nucleus ambiguus showed significant neuron loss (data not shown). Compared to the relatively diffuse neuron loss in the ION, the loss in the pontine base was especially patchy. Small groups of intact neurons were juxtaposed to similar small regions of gray matter devoid of neurons. To map the involved regions, the gliotic areas were selected by color and then blackened (Fig. 8e). Neuron loss was greatest caudally and ventrally. However, in the ventral region, the loss was greater medially and laterally, but showed relative sparing between these regions. The dorsal aspects of the pontine base, further removed from the corticospinal fibers, were only minimally involved. Commensurate with the pontine neuron loss, the middle cerebellar peduncle (MCP) was slightly pale and showed increased eosinophilia of gliosis. Similar to the ION, a few APP-positive swollen, beaded axons stained in the pontine base; these were not clustered and were rare (Fig. 8f).

Unlike the ION and pontine base, the cerebellum showed little evidence of neural degeneration. Neither the folia of the hemispheres nor the flocculus were atrophic (see Fig. 2g) or showed qualitative loss of Purkinje or internal granular neurons (Fig. 8g). The molecular layer, which degenerates following loss of these neurons, was not atrophic (Fig. 8g). Similarly, the dentate nucleus had an appropriate density of neurons and was not gliotic (Fig. 8h). The superior cerebellar peduncle (SCP), which represents the main output bundle from the dentate nucleus, was normal (see Fig. 8d). The very rare axonal torpedoes were highlighted using immunostains for neurofilament (Fig. 8i); such torpedoes were not a primary feature of this disease. Examination of an entire slide of cerebellum disclosed mild white matter pallor, especially inferiorly, which is commensurate with the moderate loss of fibers from the MCP (data not shown).

Remaining brain

The allocortex, including the amygdala, ventral claustrum, entorhinal cortex and ventral insula, were preserved. In the thalamus, the anterior nucleus displayed neuron loss and gliosis along the dorsomedial edge. The locus ceruleus and the median raphe nucleus showed mild neuronal loss. Structures lacking pathological changes included the basal ganglia, cerebellum, substantia nigra and dentate nuclei (all data in this section are not illustrated).

Discussion

This report confirms and extends published neuropathological reports of patients with Wolfram syndrome. Previous described findings, confirmed in our patient, included atrophy of the optic tracts and chiasm, atrophy of the pons and loss of neurons from the paraventricular nuclei and supraoptic nuclei of the hypothalamus [6,8,25,26]. However, in this patient, we examined the pathology of other structures, including the eye and inner ear, which had not been previously

reported. The anatomical pathology correlates well with many of the patient's symptoms. We have also identified several significant discrepancies compared with other reports.

Clinicopathological correlations

Diabetes mellitus is a key feature of Wolfram syndrome. Our patient became insulin dependent at age 12. At autopsy, his pancreas showed a marked decrease in insulin-producing pancreatic islet cells, which was confirmed by the near absence of synaptophysin immunohistochemical staining. This finding has been previously reported [12].

Diabetes insipidus is another component of Wolfram syndrome. A loss of vasopressin-producing neurons in the hypothalamus has been well documented in this disease and is thought to be the cause of Wolfram syndrome-associated diabetes insipidus [17,25]. Our patient had central diabetes insipidus and had lost most of the supraoptic and paraventricular nuclei magnocellular hypothalamic neurons that produce vasopressin. Vasopressin produced in the hypothalamus is normally transported down axons to the neurohypophysis and secreted at the axonal terminals. In our patient, the neurohypophysis was completely atrophic and reduced to a small crescent of glial tissue at the posterior of the adenohypophysis. Neuroradiologists have reported a loss of signal intensity in the posterior pituitary, indicating an absence or degeneration of the neurohypophysis [7,25]; some patients have been found to have "empty sellae" [27].

Functional tests of the pituitary have shown deficiencies in somatotropic and corticotropic function in a significant proportion of patients, indicating possible additional involvement of the anterior pituitary [3,27] or hypothalamic-releasing hormone neurons. Carson et al. [3] also described an absence of the posterior lobe of the pituitary in neuropathologic examination of one of their patients. Their study also noted bilateral adrenal atrophy, which may have been a result of pituitary dysfunction; however, this finding was not identified in our patient. Additionally, immunostains of the major anterior pituitary hormones were all positive in individual neurons, indicating expression of these hormones.

Our patient suffered from progressive blindness that began at an early age. At autopsy, his eyes showed marked degeneration of retinal ganglion neurons and concomitant axonal degeneration in his optic nerves and tracts. In addition, his inner nuclear layer had a reduced number of nuclei. Both his inner and outer plexiform layers were thin. This likely reflects the loss of intrinsic synaptic connections in the retina from a partial loss of ganglion, horizontal and bipolar cells, since his amacrine interneurons were relatively preserved in calretinin stains. His LGN also displayed neuron loss. Some retinal-geniculate axons remained in his optic tract, a few magnocellular neurons remained in his LGN, and his primary visual cortex was preserved, which suggests why he was still able to see bright light. Other studies have documented neuronal loss in the superior colliculus, although we did not appreciate this in our patient [26].

Deafness in Wolfram's syndrome is commonly a high-frequency, symmetric, sensorineural hearing loss, usually manifesting in the second or third decade with a relatively slow rate of deterioration [20,21]. Our patient fits this profile with a bilateral high-frequency hearing loss evidenced by age 12. The loss of hair cells in the basal turn of both cochleae seen in our patient correlates well with his high-frequency hearing loss, commensurate with the well-known tonotopic representation of high-frequency sounds in the basal parts of the cochlea. Immunostaining of the mouse cochlea showed strong expression of Wolframin protein in hair cells and supporting cells of the organ of Corti, as well as in cochlear neuronal cells, along with weak expression in strial marginal cells [5]. Therefore, atrophy of the organ of Corti appears to be a specific correlate of the hearing loss in Wolfram syndrome. However, the reason for the selective loss of the organ of Corti in the basal turn is unknown. The loss of cochlear

neurons in the basal turn may have occurred as a result of retrograde neural degeneration (secondary to atrophy of the organ of Corti), or as a direct result of Wolfram syndrome. It is possible that the focal strial atrophy was also a specific correlate of Wolfram syndrome. However, focal atrophy of the stria is a very common finding in a wide variety of congenital, genetic and acquired deafnesses [24]. Overall, cochlear neurons were present in near-normal numbers and the cochlear nerve appeared normal. It is well established that the cochlear neurons, the cochlear nerve and central auditory pathways are all critically important in speech discrimination [24]. Our patient had normal speech discrimination, thereby suggesting that the central auditory pathways were mildly affected or unaffected.

The bilateral osteoclast proliferations in the bony eustachian tube are intriguing. However, we have no explanation for this finding nor can we associate them with any clinical symptom. Wolfram syndrome is not known to typically cause any bony abnormalities or osteopenia. No bone disease was described in our patient's medical history or in the general autopsy, although our study did not include a histological examination of other bones. It is possible that this is simply a focal reactive process or one related to his pituitary pathology and associated endocrine dysfunction.

Our patient had several neurological deficits that are typically associated with cerebellar function. He had gaze-evoked nystagmus, impairment of his pursuit and vestibular–ocular reflex, "slurred" speech (but normal language) and deficits in one-foot stance and tandem gait. The brain's most significant external findings were the diminutive size of the pontine base and medulla, but not of the cerebellum. Microscopically, the pontine base had a complex pattern of neuron loss. On each side, the neuron loss and gliosis were greatest around the periphery of the descending corticospinal–corticopontine fibers. This complex pattern of loss is reminiscent of the somatotopic relationship between the primary somatosensory cortex and the pons, in which oral regions of the rat are represented centrally on each side, and trunk and limbs occupy progressively larger shells around the central region [14]. In our patient, the central region was relatively preserved, compared to the peripheral "shells" of neurons. In addition, the pattern of neuron loss in the pons was patchy; small clusters of neurons (20–50) lay adjacent to similar size regions of gray matter devoid of remaining neurons. The patient's inferior olivary nucleus had also lost a moderate number (about 60%) of neurons, but in a diffuse rather than patchy pattern. In contrast to these two precerebellar nuclei, the cerebellum itself did not show significant neuron loss in its input areas (internal granular neurons), Purkinje neurons or output neurons (dentate nucleus), in either the hemispheres or flocculus. Some loss of cerebellar white matter had occurred, likely the consequence of pontine neuron loss, but was difficult to quantify. Similarly, this report did not further examine mossy fiber terminals in the internal granular layer; such an examination would be complicated by the partial loss in the pons, but the preservation of the ascending spinocerebellar fibers. How our patient's complex but moderate pattern of neuron loss in the pons and ION correlate with his mild "cerebellar" symptoms remains speculative, however we feel the pathology in these structures and other medullary nuclei likely produced most of his clinical features. Given the patient's impaired vestibuloocular reflex, the lack of flocculus pathology suggests that projections from the vestibular system were damaged [19].

Genis et al. [8] reported that their patient also exhibited cerebellar symptoms such as postural tremor and unsteadiness, for which they were able to demonstrate moderate loss of neurons in the dentate nuclei of the cerebellum with a reduction in Purkinje cells. Other reports have also documented cerebellar atrophy and Purkinje cell loss [3,17]. Such changes were not significant in our patient. We did not appreciate any significant cerebellar cortical or nuclear pathology in our patient.

Substantia nigra pathology was reported by Carson et al. [3] with loss of pigment, neuronal degeneration and gliosis, but this has not been described elsewhere. Their patient did not exhibit any deficiencies in motor function. Our patient had no described bradykinesia or tremors and his substantia nigra had not degenerated.

Pathophysiology

It is unknown whether the loss of islet cells represents a primary process or a secondary one arising from an unidentified central neuropathologic defect. Beta cell loss can occur in the absence of neuronal degeneration, as has been reported in mice deficient only in beta islet cells for the Wfs1 gene [23]. No autoimmune process or HLA system involvement has been identified [1,12,18]. The defective wolframin protein, which is expressed in islet cells, is likely to be involved in pancreatic beta cell loss due to its proposed role in cellular stress relief [10].

The pathology in our patient involved seemingly disparate neuronal types involving several anatomically and functionally separated systems. The affected systems included special sensory systems (vision, auditory, possibly vestibular), olivopontine system and several endocrine systems (insulin, vasopressin, likely oxytocin). Intriguingly, our patient was diagnosed with Hashimoto's thyroiditis at the age of 11; whether this represents dysfunction in an additional endocrine system remains speculative. How these three different types of systems are related in Wolfram's syndrome is unknown.

Given the genetic basis for this patient's disease, the question arises whether the primary pathology arose during development or resulted from cellular degeneration. Clinically, the patient lost milestones throughout his childhood and adolescence, indicating that the systems were intact and later degenerated. Examination of his brain revealed cellular loss and gliosis in intact nuclei and secondary axonal degeneration, rather than absence or malformation of the affected structures. The ears showed a gradual, but focally complete, loss of the organ of Corti as one progresses down the cochlea. This gradation of loss and the patient's clinical history suggest a progressive pathology of a once essentially normal ear structure and function. Overall our findings, in conjunction with previous neuropathological reports, indicate that Wolfram syndrome is predominantly a neurodegenerative process affecting multiple select systems, a process that begins early in childhood and continues throughout the life of the individual. In our patient, we cannot completely exclude a congenital component, since the atrophy in select regions of his brain (pons, medulla) seemed out of proportion to his neuronal loss.

Shannon et al. [26], in addition, noted swollen and dystrophic axons in numerous locations including the pons, fornix and certain areas in the deep cerebral white matter. Despite careful inspection, no axonal pathology was identified on routine stains. Staining for amyloid precursor protein, which is a marker for active axonal injury, showed only occasional axons in the pontine base and ION. Stains for neurofilament disclosed only a few torpedoes in the cerebellar internal granular layer over an entire region sampled. Using silver stains, no axonal spheroids were identified in the primary visual cortex. Primary axonal pathology was not a feature of our patient. We cannot fully explain the discrepancy between our results and those of Shannon et al.

The LGN is well known to undergo transsynaptic degeneration following unilateral or bilateral loss of an eye or vision. The LGN in our patient had undergone massive neuron loss and gliosis. However, our data are mute concerning whether the loss represents transsynaptic degeneration or a primary neurodegenerative process. Given the patient's intact cochlear nucleus and other primary sensory nuclei, we favor transsynaptic degeneration.

Unexamined topics and unexplored areas

Several phenomena in this patient have not been further characterized. The anterior pituitary had focal fibrosis and focal loss of cellular architecture, which are of uncertain significance. Whether these findings as a whole indicate damage to the hypothalamus with secondary degenerative changes of the pituitary or primary pituitary disease is unclear. Genis et al. [8] reported olfactory bulb and tract atrophy in a case of Wolfram syndrome with anosmia. We did not microscopically examine our patient's olfactory system, although grossly the olfactory tracts and bulbs were not decreased in size. We have also not examined in detail the different subtypes of neurons in the retina. Our patient expired from repeated bouts of pneumonia that were likely related to central hypoventilation. While we observed neuron loss in medullary reticular formation, we did not map this further. In addition, we noted neuron loss in the medial vestibular nucleus, but did not further characterize the vestibular system. Although mossy fibers from the pons should have shown some degeneration in the cerebellar internal granular layer, we did not investigate this further. Similarly, axons projecting from the LGN to layer IV-C of the primary visual cortex should have degenerated; this was not further examined. We also did not examine subcortical visual systems. Finally, the patient suffered from clinical depression and occasional bouts of suicidal ideation. Although his entire brain was small (1,100 g compared to 1,400 g for normal male adult), we could not qualitatively identify pathology in neocortical or limbic regions. Subtle loss of neurons in any region would have been difficult to detect in this autopsy analysis.

Conclusion

This report confirms features of Wolfram's syndrome that have been described by others, including atrophy of the optic nerves and tract, loss of neurons from the supraoptic and paraventricular nuclei and atrophy of the basal pons [3,8,11,13,26]. Additionally, we have provided more detailed descriptions of the visual, auditory, hypothalamic-pituitary and the olivopontocerebellar system pathology. Our findings imply that the major pathology in patients with Wolfram's disease is due to neuron cell loss, rather than congenital development or axonal pathology. We also feel that the detailed anatomical investigations in this patient have heuristic education value, since many of the neuroanatomic systems involved in Wolfram's syndrome are typically only briefly covered or covered only once in the education of a physician. We recognize that several major questions or areas of investigation remain in our understanding of this devastating neurodegenerative disease.

Acknowledgments

The authors would like to express their sincere thanks to the patient's family for allowing us to conduct this study. We especially would like to thank the patient's mother who has been of invaluable assistance in providing pertinent medical records and overall inspiration. Supported by NIH (U24 DC 008559), Mr. Lakshmi Mittal and Mr. Axel Eliasen.

References

1. Barrett TG, Bundy SE, Macleod AF. Neurodegeneration and diabetes: UK nationwide study of Wolfram (DIDMOAD) syndrome. Lancet 1995;346:1458–1463. [PubMed: 7490992]doi: 10.1016/S0140-6736(95) 92473-6
2. Barrett TG, Bundy SE, Fielder AR, Good PA. Optic atrophy in Wolfram (DIDMOAD) syndrome. Eye 1997;11:882–888. [PubMed: 9537152]
3. Carson MJ, Slager UT, Steinberg RM. Simultaneous occurrence of diabetes mellitus, diabetes insipidus, and optic atrophy in a brother and sister. Am J Dis Child 1977;131:1382–1385. [PubMed: 930889]

4. Chiquet C, Dkhissi-Benyahya O, Cooper HM. Calcium-binding protein distribution in the retina of strepsirhine and haplorhine primates. Brain Res Bull 2005;68:185–194. [PubMed: 16325019]doi: 10.1016/j.brainresbull.2005.08.010
5. Cryns K, Thys S, Van Laer L, Oka Y, Pfister M, Van Nassauw L, Smith RJ, Timmermans JP, Van Camp G. The WFS1 gene, responsible for low-frequency sensorineural hearing loss and Wolfram syndrome, is expressed in a variety of inner ear cells. Histochem Cell Biol 2003;119:247–256. [PubMed: 12649740]
6. Domenech E, Gomez-Zaera M, Nunes V. Wolfram/DIDMOAD syndrome, a heterogenic and molecularly complex neurodegenerative disease. Pediatr Endocrinol Rev 2006;3:249–257. [PubMed: 16639390]
7. Galluzzi P, Filosomi G, Vallone IM, Bardelli AM, Venturi C. MRI of Wolfram syndrome (DIDMOAD). Neuroradiology 1999;41:729–731. [PubMed: 10552021]doi:10.1007/s002340050832
8. Genis D, Davalos A, Molins A, Ferrer I. Wolfram syndrome: a neuropathological study. Acta Neuropathol 1997;93:426–429. [PubMed: 9113209]doi:10.1007/s004010050635
9. Inoue H, Tanizawa Y, Wasson J, et al. A gene encoding a transmembrane protein is mutated in patients with diabetes mellitus and optic atrophy (Wolfram syndrome). Nat Genet 1998;20:143–148. [PubMed: 9771706]doi:10.1038/2441
10. Ishihara H, Takeda S, Tamura A, et al. Disruption of the *WFS1* gene in mice causes progressive β-cell loss and impaired stimulus–secretion coupling in insulin secretion. Hum Mol Genet 2004;13:1159–1170. [PubMed: 15056606]doi:10.1093/hmg/ddh125
11. Jackson MJ, Bindoff LA, Weber K, et al. Biochemical and molecular studies of mitochondrial function in diabetes insipidus, diabetes mellitus, optic atrophy, and deafness. Diabetes Care 1994;17:728–733. [PubMed: 7924787]doi:10.2337/diacare.17.7.728
12. Karasik A, O'Hara C, Srikanta S, et al. Genetically programmed selective islet beta-cell loss in diabetic subjects with Wolfram's syndrome. Diabetes Care 1989;12:135–138. [PubMed: 2649325]doi: 10.2337/diacare.12.2.135
13. Khardori R, Stephens JW, Page OC, Dow RS. Diabetes mellitus and optic atrophy in two siblings: a report on a new association and a review of the literature. Diabetes Care 1983;6:67–70. [PubMed: 6839924]doi:10.2337/diacare.6.1.67
14. Leergaard TB, Lyngstad KA, Thompson JH, et al. Rat somatosensory cerebropontocerebellar pathways: spatial relationships of the somatotopic map of the primary somatosensory cortex are preserved in a three-dimensional clustered pontine map. J Comp Neurol 2000;422:246–266. [PubMed: 10842230]doi: 10.1002/(SICI)1096-9861(20000626)422:2<246::AID-CNE7>3.0.CO;2-R
15. Lund J. Organization of neurons in the visual cortex, area 17, of the monkey (*Macaca mulatta*). J Comp Neurol 1973;147:455–496. [PubMed: 4122705]doi:10.1002/cne.901470404
16. Lund JS. Anatomic organization of Macaque monkey striate visual cortex. Annu Rev Neurosci 1988;11:253–288. [PubMed: 3284442]doi:10.1146/annurev.ne.11.030188.001345
17. Medlej R, Wasson J, Baz P, et al. Diabetes mellitus and optic atrophy: a study of Wolfram syndrome in the Lebanese population. J Clin Endocrinol Metab 2004;89:1656–1661. [PubMed: 15070927]doi: 10.1210/jc.2002-030015
18. Monson JP, Boucher BJ. HLA type and islet cell antibody status in families with (diabetes insipidus and mellitus, optic atrophy, and deafness) DIDMOAD syndrome. Lancet 1983;1(8336):1286–1287. [PubMed: 6134087]doi:10.1016/S0140-6736(83)92746-0
19. Nagao S, Kitamura T, Nakamura N, Hiramatsu T, Yamada J. Differences of the primate flocculus and ventral paraflocculus in the mossy and climbing fiber input organization. J Comp Neurol 1997;382:480–498. [PubMed: 9184995]doi: 10.1002/(SICI)1096-9861(19970616)382:4<480::AID-CNE5>3.0.CO;2-Z
20. Pennings RJ, Huygen PL, van den Ouweland JM, et al. Sex-related hearing impairment in Wolfram syndrome patients identified by inactivating WFS1 mutations. Audiol Neurootol 2004;9:51–62. [PubMed: 14676474]doi:10.1159/000074187
21. Plantinga RF, Pennings RJ, Huygen PL, Bruno R, Eller P, Barrett TG, Vialettes B, Paquis-Fluklinger V, Lombardo F, Cremers CW. Hearing impairment in genotyped Wolfram syndrome patients. Ann Otol Rhinol Laryngol 2008;117:494–500. [PubMed: 18700423]

22. Polymouropoulos M, Swift R, Swift M. Linkage of the gene for Wolfram syndrome to markers on the short arm of chromosome 4. Nat Genet 1994;8:95–97. [PubMed: 7987399]doi: 10.1038/ng0994-95

23. Riggs AC, Bernal-Mizrachi E, Ohsugi M, Wasson J, Fatrai S, Welling C, Murray J, Schmidt RE, Herrera PL, Permutt MA. Mice conditionally lacking the Wolfram gene in pancreatic islet beta cells exhibit diabetes as a result of enhanced endoplasmic reticulum stress and apoptosis. Diabetologia 2005;48:2313–2321. [PubMed: 16215705]doi:10.1007/s00125-005-1947-4

24. Schuknecht, HF. Pathology of the ear. Vol. 2nd edn.. Philadelphia: Lea and Febiger; 1993.

25. Scolding NJ, Kellar-Wood HF, Shaw C, Shneerson JM, Anton Nagui. Wolfram syndrome: hereditary diabetes mellitus with brainstem and optic atrophy. Ann Neurol 1996;29:352–360. [PubMed: 8602754]doi:10.1002/ana.410390312

26. Shannon P, Becker L, Deck J. Evidence of widespread axonal pathology in Wolfram syndrome. Acta Neuropathol 1999;98:304–308. [PubMed: 10483789]doi:10.1007/s004010051084

27. Soliman AT, Bappal B, Darwish A, Rajab A, Asfour M. Growth hormone deficiency and empty sella in DIDMOAD syndrome: an endocrine study. Arch Dis Child 1995;73:251–253. [PubMed: 7492167] doi:10.1136/adc.73.3.251

28. Strom TM, Hortnagel K, Hofmann S, et al. Diabetes insipidus, diabetes mellitus, optic atrophy and deafness (DIDMOAD) caused by mutations in a novel gene (wolframin) coding for a predicted transmembrane protein. Hum Mol Genet 1998;7:2021–2028. [PubMed: 9817917]doi: 10.1093/hmg/7.13.2021

29. Turnbridge RE, Paley RG. Primary optic atrophy and diabetes mellitus. Diabetes 1956;5:295–296. [PubMed: 13356719]

30. Wässle H, Grünert U, Chun M-H, Boycott BB. The rod pathway of the Macaque monkey retina: identification of AII-amacrine cells with antibodies against calretinin. J Comp Neurol 1995;361:537–551. [PubMed: 8550898]doi:10.1002/cne.903610315

31. Wolfram DJ, Wagener HP. Diabetes mellitus and simple optic atrophy among siblings: report of four cases. Mayo Clin Proc 1938;9:715–718.

32. Zatyka M, RickMinton J, Fenton S, et al. Sodium–potassium ATPase 1 subunit is a molecular partner of Wolframin, an endoplasmic reticulum protein involved in ER stress. Hum Mol Genet 2008;17:190–200. [PubMed: 17947299]doi:10.1093/hmg/ddm296

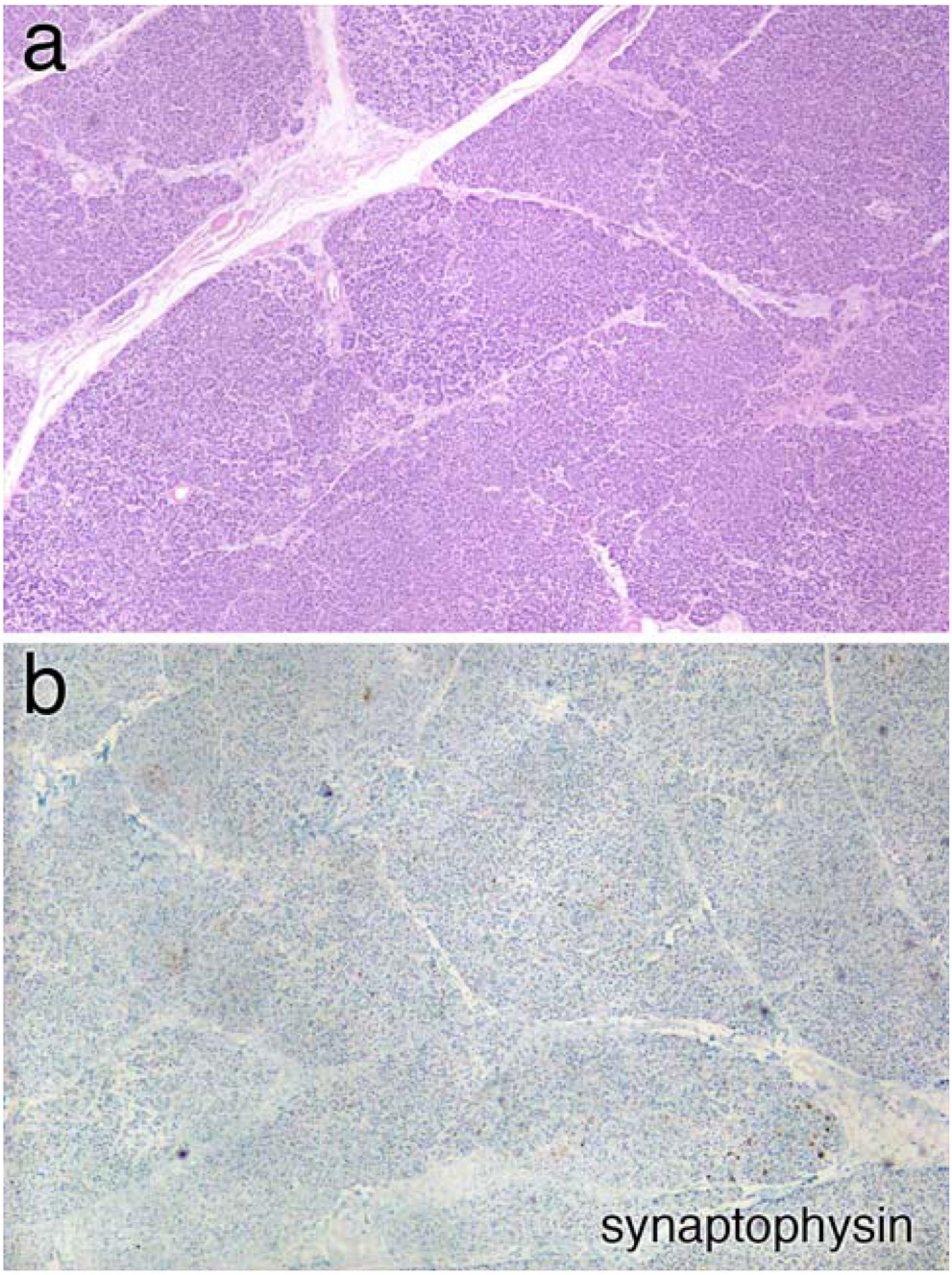

Figure 1.

Pancreas pathology. **a** Medium magnification view of the pancreas stained with hematoxylin and eosin (H&E). The organ has a normal lobular architecture; however no small, pale islands containing islets cells are visible. This is confirmed in panel (**b**), which has been immunostained with synaptophysin; no islands of islets cells are identified

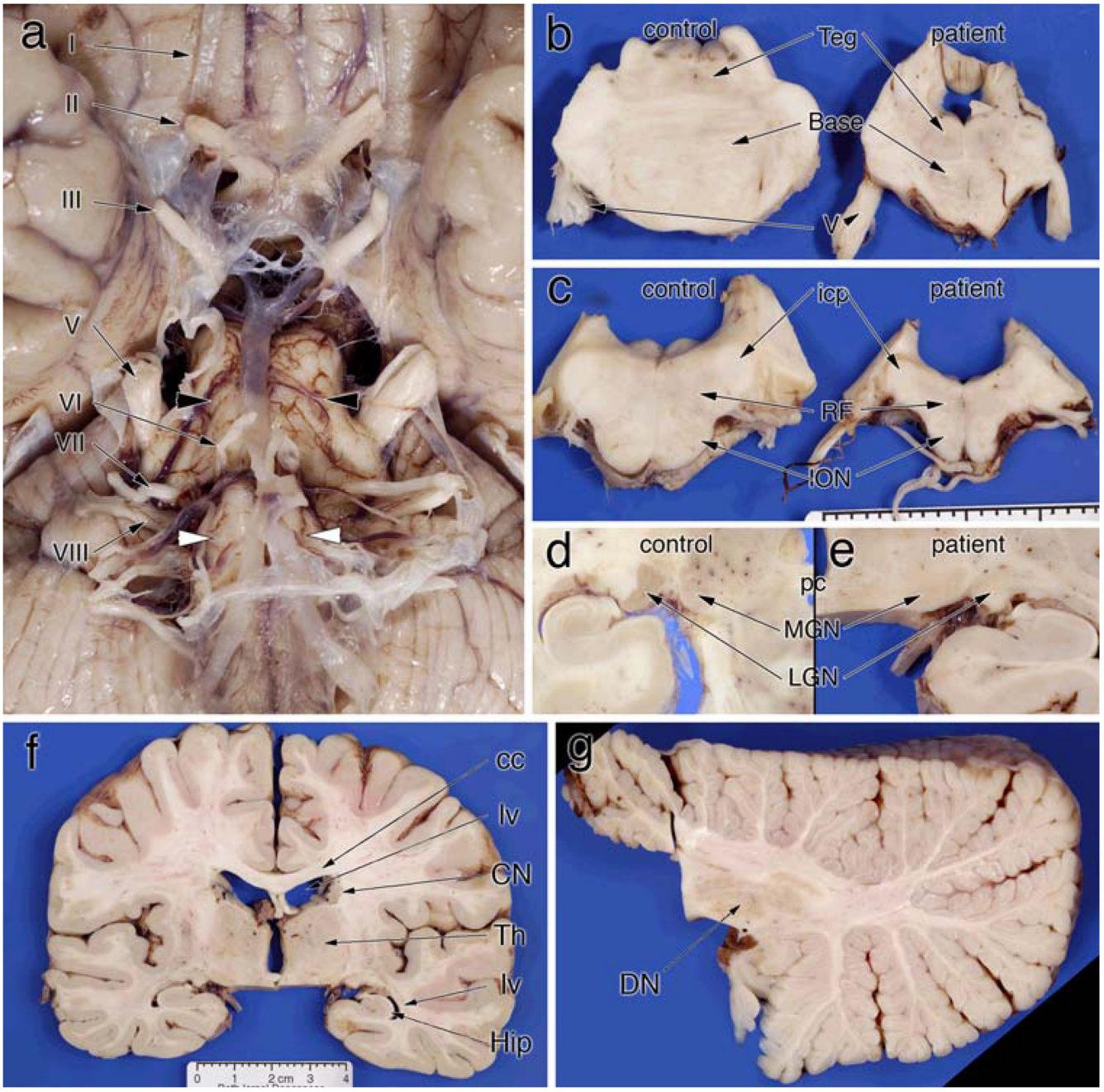

Figure 2.

Gross pathology. **a** Ventral view of the brainstem and optic nerves. The optic nerve (II) has a light brown color, rather than white, and has shrunken almost to the size of the oculomotor nerve (III). The remaining cranial nerves are unremarkable (IV–VIII). However, both the medulla (*white arrowheads*) and pons (*black arrowheads*) are significantly shrunken. **b** The diminution of the pontine base compared to a normal control. While the tegmentum (*teg*) has a normal height, the base is significantly smaller in all dimensions. **c** Similarly illustrates changes in the rostral medulla at the level of the inferior cerebellar peduncle (*icp*). The inferior olivary (*ION*) bulge is flattened and the medullar reticular formation (*RF*) is small. **d** A normal lateral geniculate nucleus (*LGN*) and medial geniculate nucleus (*MGN*) at the level of the

posterior commissure (*pc*). **e** In the patient, the MGN has the same light gray color as the control; in contrast, the LGN completely lacks the darker brown color of the control. The coronal section in (**f**), which includes the LGN in (**e**), illustrates the essentially normal telencephalon. The lateral ventricles (*lv*) are not dilated, the corpus callosum (*cc*) is not atrophic or discolored, the thalamus (*Th*) is of normal size and configuration (except for the pallor in the LGN), and no hippocampal (*Hip*) shrinkage is present. Similarly, the radial section of the cerebellum in (**g**) displays no atrophy of the folia, and the dentate nucleus (*DN*) has a normal size and color

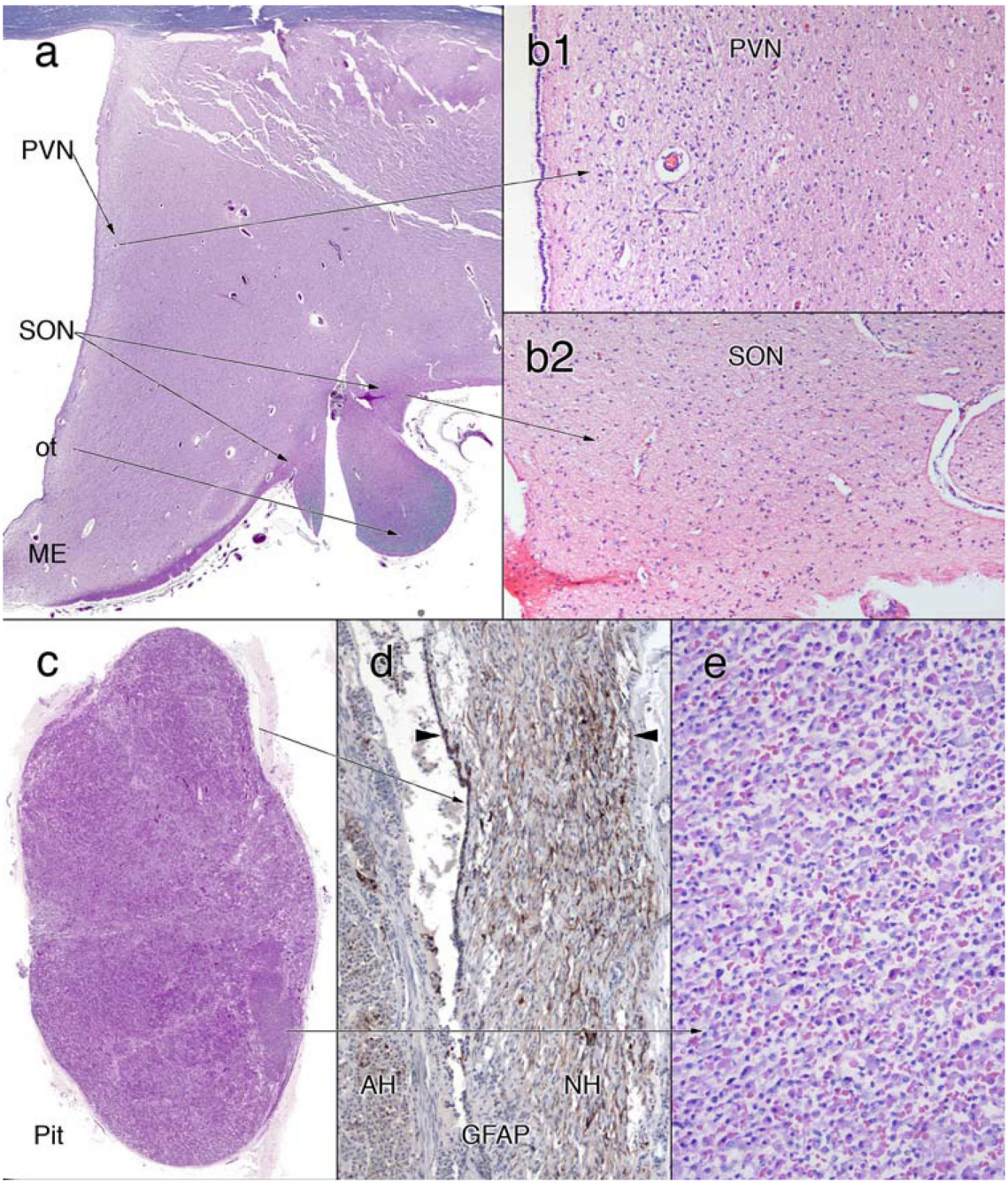

Figure 3.

Hypothalamus–pituitary axis. **a**–**c** H&E/LFB stains, **c**, **e** are H&E stains, **d** an immunostain for glial fibrillary acidic protein (*GFAP*). The coronal section of the hypothalamus in panel (**a**) is a field view showing the locations of the paraventricular (*PVN*) and supraoptic (*SON*) nuclei. The median eminence (*ME*) is preserved while the optic tract (*OT*) has lost most of its central myelinated axons. The large neurons with peripherally marginated Nissl that characterized the PVN (**b1**) and SON (**b2**) are absent in these sites. The pituitary in (**c**) lacks a normal neurohypophysis; serial sections through the remaining pituitary were similar. Immunostains for GFAP in (**d**) show that the small rim of eosinophilic material in (**c**) represents a remnant of the posterior pituitary. The entire neurohypophysis is confined to a narrow band

(*between the arrowheads*) at the posterior of the adenohypophysis. A small area of the pituitary that lacks normal architectural nesting in (**c**) (*origin of arrow*) still retains a normal complement of eosinophilic, basophilic and amphophilic cells (**e**)

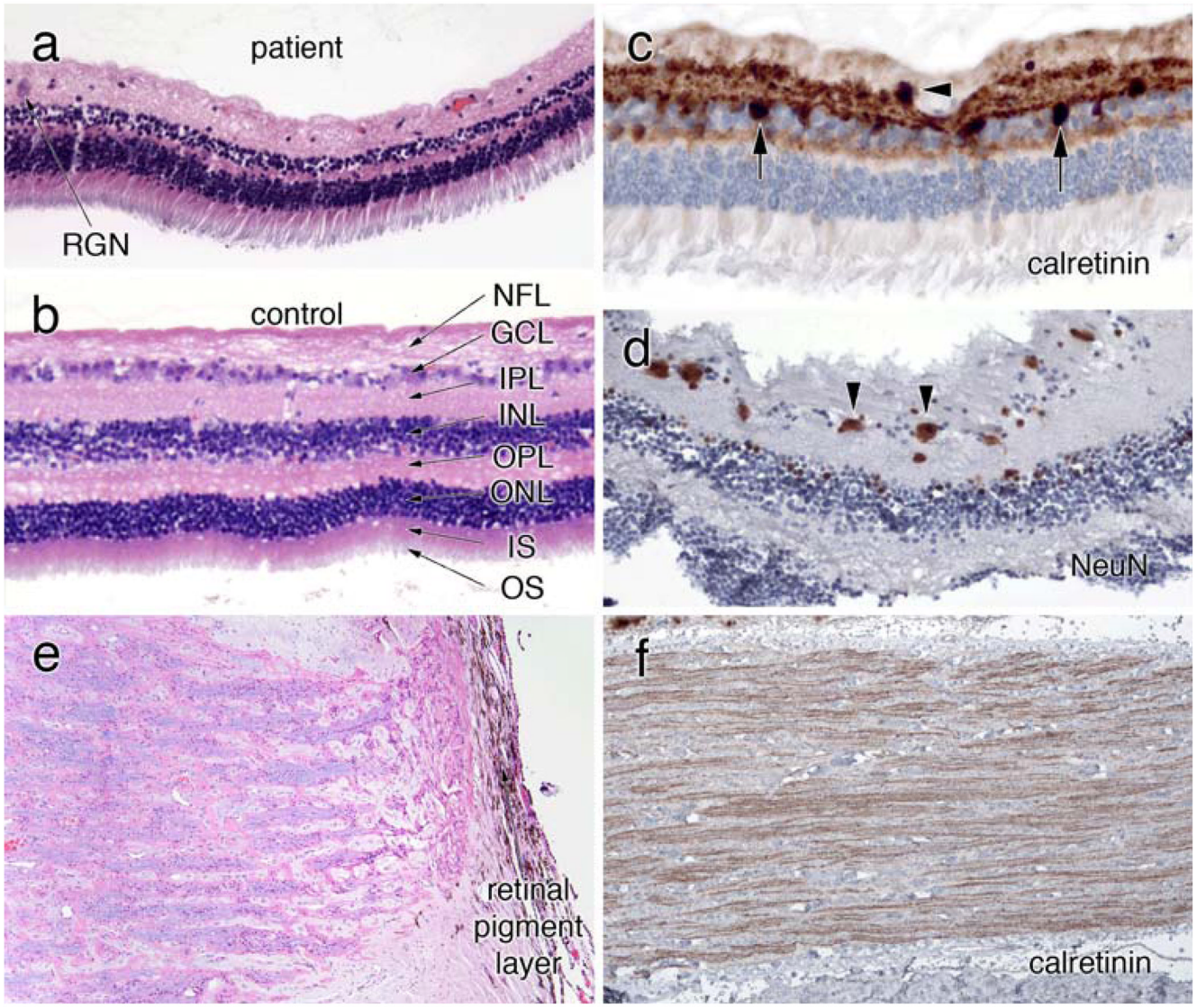

Figure 4.

Eye. **a**, **b** Compare the retinal histology (H&E) in the patient and a control retina. They are at the same magnification, as determined by the similar width of the rod inner and outer segment layers. The patient's retina has very few remaining retinal ganglion neurons (RGN) in the ganglion cell layer (*GCL*). Neurons in the inner (*INL*) and outer (*ONL*) neuronal layers are relatively preserved, while both the inner (*IPL*) and outer (*OPL*) plexiform layers are greatly diminished. **c** Stained for calretinin and shows an occasional RGN in the GCL (*black arrowhead*). Some calretinin-positive cells lie within the inner aspect of the INL. The Neu-N immunostain in (**d**), which reacts with a subset of neurons, reveals more RGN (*black arrowheads*), several of which are small or shrunken. **e** is an H&E-Luxol fast blue (H&E/LFB) stain of the head of the optic nerve. Many of the ganglion neuron axons have degenerated, resulting in pale myelin staining. Calretinin immunostains in (**f**) highlight remaining retinogeniculate axons

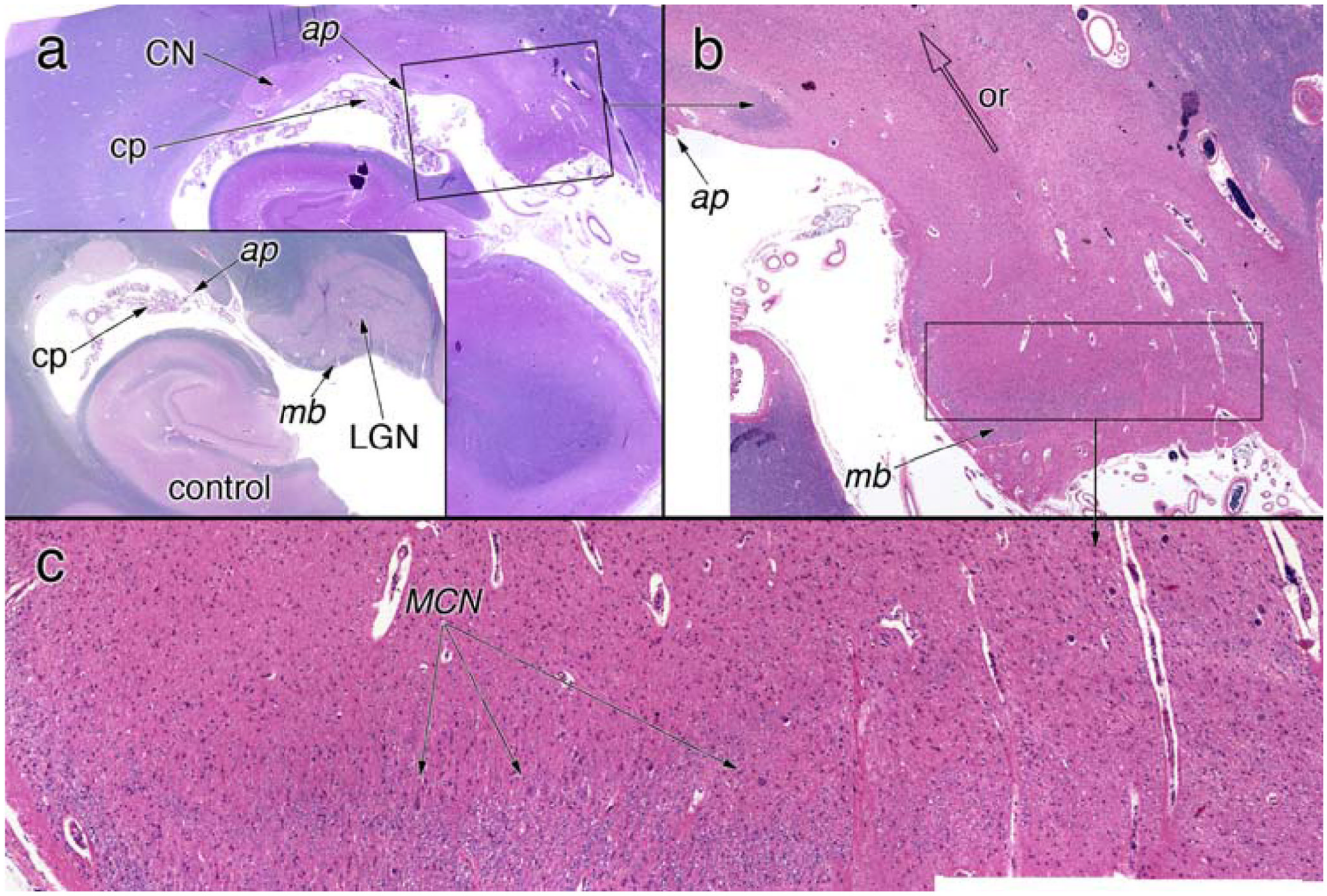

Figure 5.

Lateral geniculate nucleus. **a** A low-magnification view of the hippocampus and lateral geniculate nucleus (*LGN*). For orientation, the *inset* shows a normal LGN. Notice that the LGN lies medial to the attachment point (*ap*) of the choroid plexus (*cp*), while the tail of the caudate nucleus (*CN*) is lateral to this point. In the control, the LGN is completely surrounded by myelinated axons; a myelin boundary (*mb*) separates the LGN from the surface of the brain. **b** A higher magnification view of the LGN, from the *box* in (**a**). This image is a composite of multiple smaller images taken at higher magnification and then combined to give higher resolution. The LGN lacks any discernable six-layer structure (see the control LGN). The optic radiation (*or*) is completely devoid of myelinated axons. A small amount of myelin is present in the myelin boundary (*mb*). **c** A higher magnification view from the *box* in (**b**). A few remaining magnocellular neurons (*MCN*, *arrows*) lie immediately superior to the myelinated axons; however, most neurons in the LGN are absent

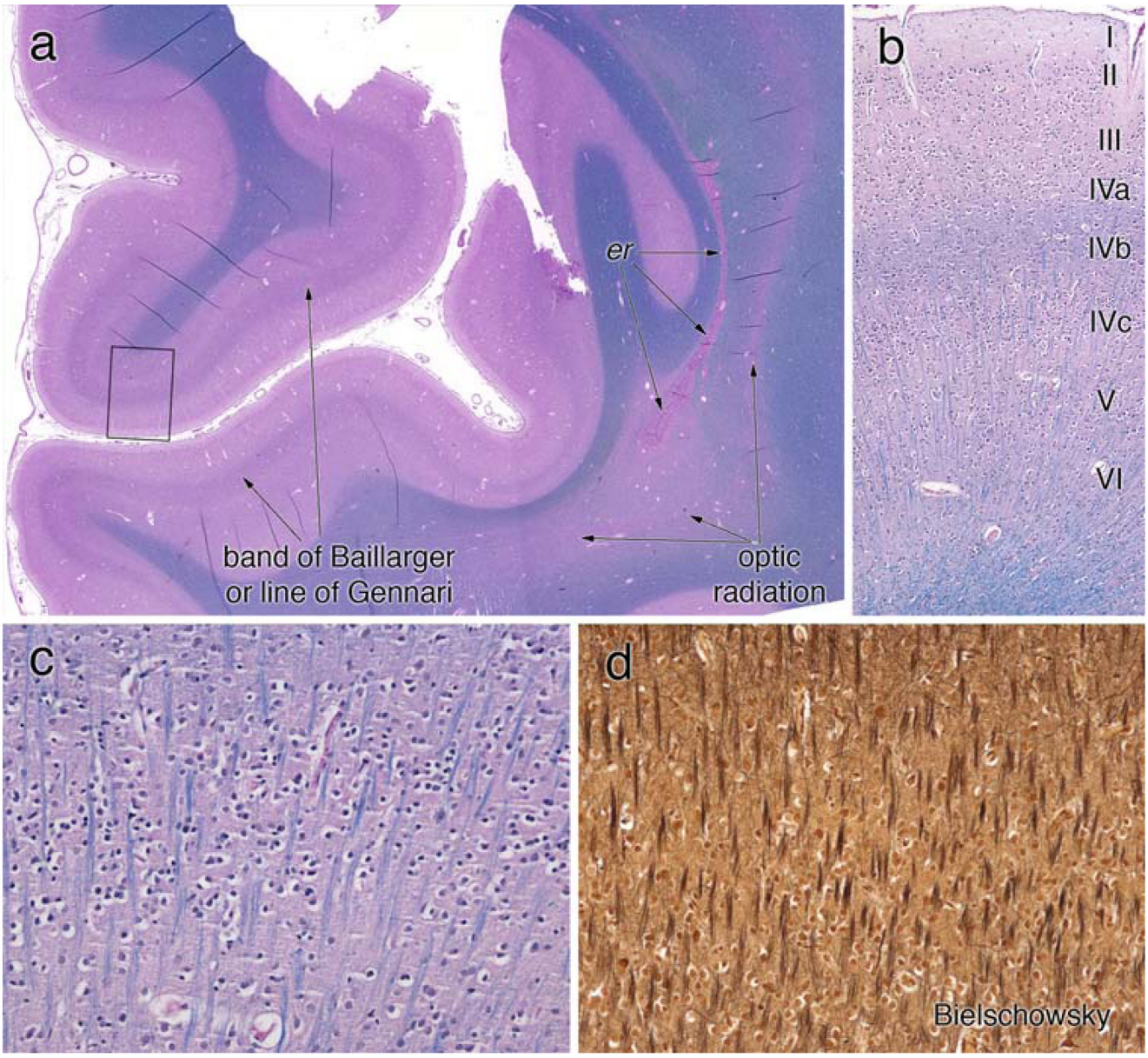

Figure 6.

Primary visual cortex. The coronal section of the primary visual cortex, stained with H&E/LFB, is illustrated in a field view in (**a**). The prominent white matter band within area 17 on gross inspection is composed of well-myelinated axons (line of Gennari or outer band of Baillarger). The optic radiation, which arose from the LGN and traveled lateral to the occipital horn of the lateral ventricle, exhibits pale myelin staining in this section, in keeping with the loss in the LGN. In this patient, the posterior recesses of the lateral ventricle had closed and left a line of ependymal rests (*er*). The small *box* in (**a**) is magnified in panel b to show the cortical layers. The outer band of Baillarger, representing intracortical connections, is well myelinated in layer IV-B. Small stellate or granular neurons in IV-C are present. Layer IV-C is illustrated at high magnification in (**c**) and (**d**). Radially oriented myelinated axons are identified on both the LFB (**c**) and Bielschowsky (**d**) stains. Neither stain shows myelin ovoids

or axonal spheroids. Layer IV-C (and less so layer IV-A) is the major input lamina for the LGN; in this patient within the scope of this analysis, they are histologically normal

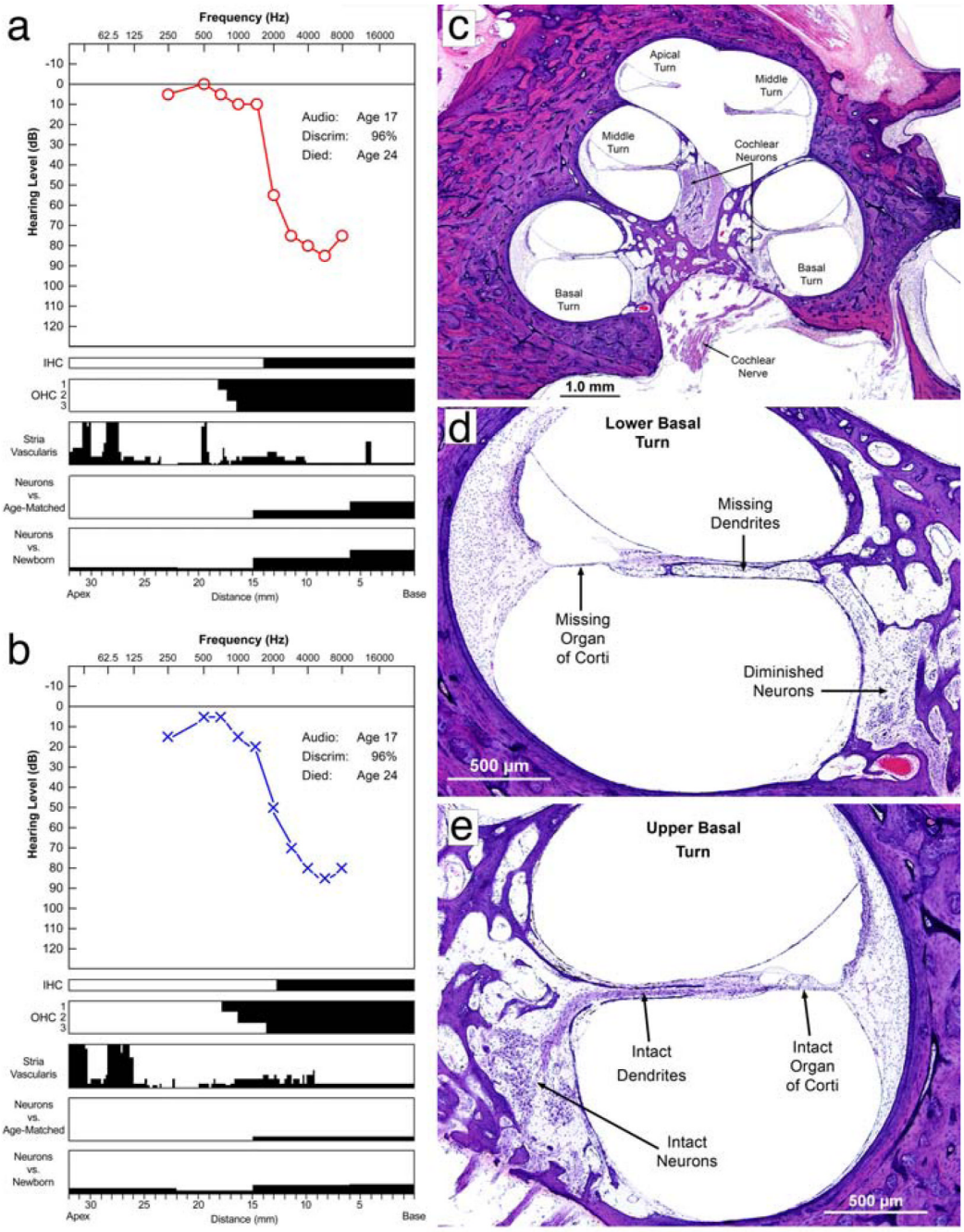

Figure 7.

Auditory system. **a, b** Audiogram along with a quantitative analysis of neurosensory elements within the cochleae. Audiometric thresholds in the right and left ears at age 17 are shown in (**a**) and (**b**), respectively. Speech discrimination was 96% in both ears (normal). The cytologic alterations are displayed below the audiogram in a series of *parallel bar graphs*, with distance in millimeters from the basal end on the *x* axis from *right* to *left*, and magnitude of pathologic changes on the *y* axis (*black*) from *bottom* to *top*. The composite graph is known as the cytocochleogram [24]. This method allows depiction of the pathologic changes and its correlation with the associated audiogram. By displaying the pathology and the audiometric results on the same scale, the tonotopic organization of the cochlea is incorporated, and one

can correlate the site of pathology (e.g., hair cell loss) with the frequency distribution of the hearing loss (on the audiogram). The *black areas* in the cytocochleogram represent missing or abnormal elements. The inner and outer hair cells are shown as present (*white*) or absent (*black*). *Vertical axes* of the cytocochleogram for the stria vascularis and cochlear neurons represent percentage of loss. The cochlear neuronal counts were compared with mean counts from normal newborns as well as age-matched control samples. It is evident that there was complete loss of inner hair cells and outer hair cells in the basal 0–13 mm of both cochleae, which corresponds well with the high-frequency sensorineural hearing loss. Note that the atrophy of the stria vascularis was focal and restricted mainly to the apical turn. The cochlear neurons were intact except in the base, where there was a mild loss. **c** A medium magnification H&E view of the cochlea at the mid-modiolar level, showing the basal, middle and apical turns. Note that the turns are fully developed. **d, e** Higher power H&E views of two of the cochlear turns. **d** The lower basal turn where the organ of Corti is completely atrophic with missing hair cells and missing supporting cells. The cochlear neurons innervating this part of the organ of Corti are also reduced in number with absence of the dendrites between the cell bodies and the organ of Corti. **e** A higher power view of the upper basal turn where the organ of Corti is intact, including outer and inner hair cells and supporting cells. There is neural innervation of the organ of Corti and the cochlear neurons are present, with dendrites extending from the cell bodies to the organ of Corti

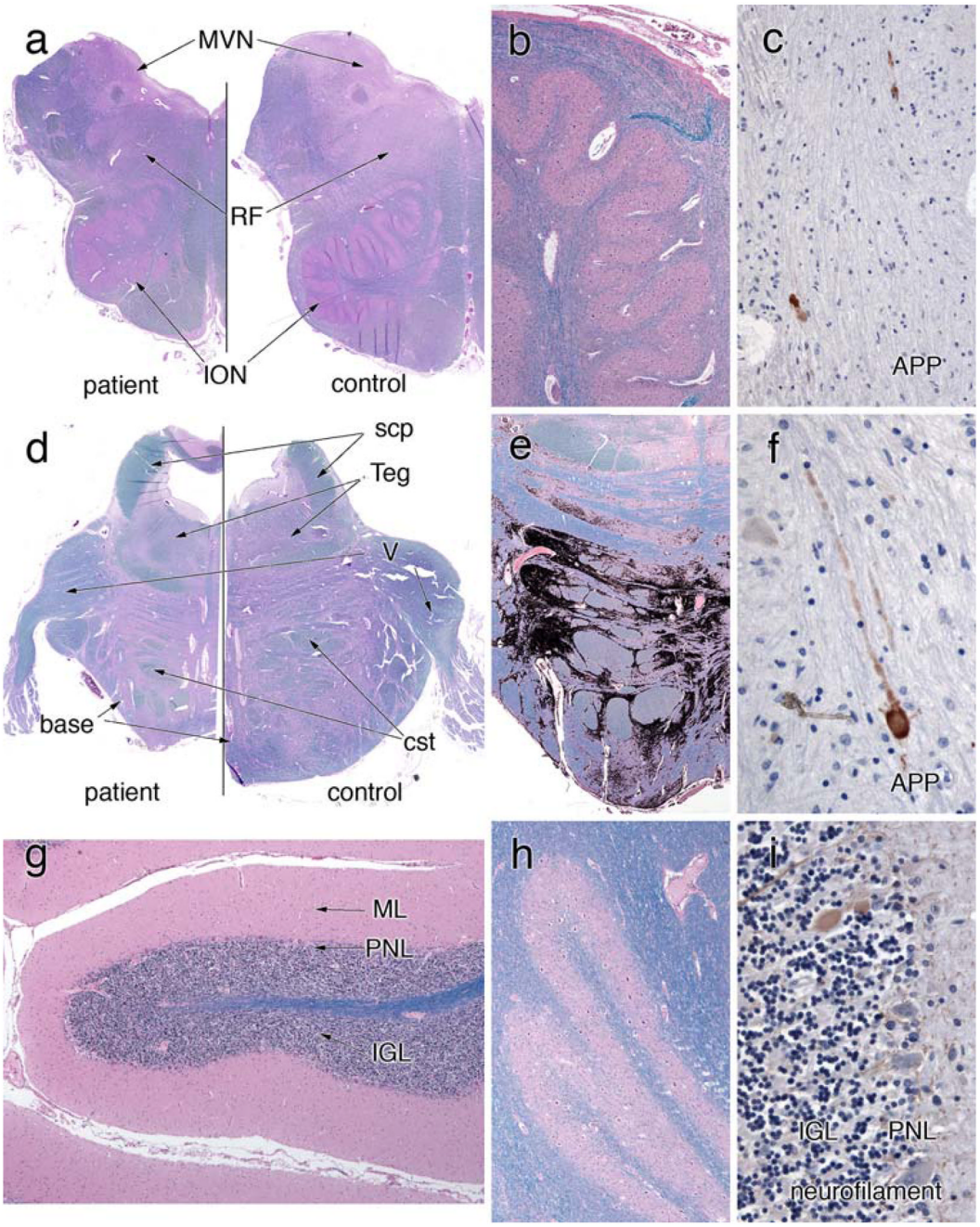

Figure 8.

Olivopontocerebellar system. **a** An H&E/LFB-stained section that compares the patient's rostral medulla with a control. The patient's entire medulla is small. Volume has been lost in the inferior olivary nucleus (*ION*) and reticular formation, and the medial vestibular nucleus (*MVN*) is slightly red, which represents a gliotic reaction to neuron loss. A higher magnification view of the ION in (**b**) reveals many remaining neurons; however, they are at a lower density than normal (see "Results"). They appear more spread out and do not show large patches of loss. Rare axons immunostain for amyloid precursor protein (*APP*) in (**c**). Similar to the medulla, the pons from the patient in (d) is small compared to the control. The tegmentum (Teg) has nearly the same size in both, but the base is moderately shrunken. The trigeminal

nerve (*V*) is similar in both. To illustrate the patchy pattern of loss in the pontine base, the more gliotic regions were color-selected and then blackened (**e**). In these patches of gliosis, neurons are lost; in adjacent gray matter regions, they are spared. Notice that the dorsal aspect of the pontine base displays only slight involvement. As in the medulla, a few APP-immunoreactive axons are present in the pontine base white matter (**f**); these are rare. **g, h** H&E/LFB stains that illustrate the normal histology of the cerebellar gray matter. The molecular layer (*ML*) is not atrophic, the Purkinje neurons layer (*PNL*) has an appropriate number of large neurons, and the internal granular layer is normal. The dentate nucleus has a normal contingent of neurons. Correlating with the normal dentate nucleus, the superior cerebellar peduncle (*scp*) in (**d**) is fully myelinated, compared to the control. A neurofilament immunostain in (**i**) highlights only very rare axonal torpedoes in the IGL (*brown-staining oval*)